The 5th International Conference on Electrical Engineering – Boumerdes (ICEE-B)
October 29-31, 2017, Boumerdes, Algeria.

Analytical Identification of the Differential Mode Impedance of a Cell Buck DC-DC Converter

Djelloul BENSAAD[1,2], Abdelchafik HADJADj[1]
[1]Laboratoire d'Analyse et de Commande des Systèmes(LACoSERE), Université Amar Telidji
Laghouat, Algeria
bensaadd@gmail.com; ahadjadjdz@yahoo.fr

Achour ALES [2]
[2]Laboratoire Systèmes Electrotechniques,
Ecole Militaire Polytechnique
Algiers, Algeria
Achour.ales@gmail.com

Abstract— **In this paper, we propose a method for identifying the differential mode impedance of a paralleled converter cell.The equivalent Thevenin / Norton circuit method is used for prediction. The predict of ElectroMagnetic Interference (generated by converters connected to the electrical network to identify the sources of noise, impedance and harmonics according to the identification of the contribution of impedances to the improvement of filters which are considered as filter charges (upstream and downstream filter side). The model is tested by the PSpice simulation with a broad range of frequencies up to 30 MHz.**

Keywords-component; modelling, differential mode, harmonic input impedance,* converter cell, *EM disturbances, switching.

I. INTRODUCTION

Scalable in all industrial fields because their integration has increased efficiency [1]. Moreover, facilitating the control of industrial systems; This advantage has also given rise to new problems related to ElectroMagnetic Interference(EMI) between these units.

In the automotive industry, the power grid has become more complex to optimise and structure [2] due to the increase in switching mode converters that rebuild small networks. One of the new challenges in the design of modern integrated electrical systems is the study of its overall ElectroMagnetic Compatibility (EMC) behaviour and the development of optimal filters, taking into account the complex environment [3].

The impedance of the converter depends on many parameters, such as converter topology, nominal power, parasitic elements of the components and board layout [3], [4], [5],[6].

Behavioural models are developed in [7] and [8] and are based on generic electrical systems given by passive components associated with voltage or current sources. In [9] and [10], modelling of N-switching cells was performed, and then a generic DM model of a buck converter was developed using a switching function.

Also, the linear invariant (LTI) has been reported and discussed here to verify the technical validity [6].

This article begins by estimating the DC-DC converter cell impedances connected in parallel to the network. These impedances are in turn used to determine the integrity of the system impedances.

This article deals in three sections:

- Identification of electromagnetic compatibility.
- Simulation PSpice impedance MD.
- Mathematical Modeling.

This study offers the designer an electromagnetic perturbation prediction by mathematical models and gives a better optimisation of the differential mode filters of the small network. More than provides an idea on ElectroMagnetic Interference (EMI) between the units of the system cell.

II. ANALYTICAL MODELING

Converters under certain conditions are linear as a function of time Invariant System (LTI), as mentioned in [6]. Based on this assertion, they could be modelled by an equivalent Norton / Thevenin circuit.[13]

A. Input Impedance Term of the Buck

The study is carried out on a cell of the DC-DC converter (Fig. 1). As it uses the switching principle, its operation is nonlinear and discontinuous. To model this process and to overcome this discontinuity, we introduce a periodic mathematical function T_{sw} to express the output signals as a function $g_{sw}(t)$ of the input variables. Also, the principle for calculating the impedance Z_{DM} consists in injecting, in differential mode, a sinusoidal voltage $v_p(t)$ expressed in (1) with $\omega_p = 2\pi f_p$ frequency at the input terminals of the converter cell, is recorded on each Converter to illustrate the curves of each and compare it with the overall impedance.

$$v_p(t) = \frac{e^{j\omega_p t} - e^{-j\omega_p t}}{2j} \quad (1)$$

$$Z_{DM} = \frac{v_p(t)}{i_p(t)} \quad (2)$$

$$i_p(t) = i_{p1}(t) + i_{p2}(t) + i_{p3}(t) \quad (3)$$

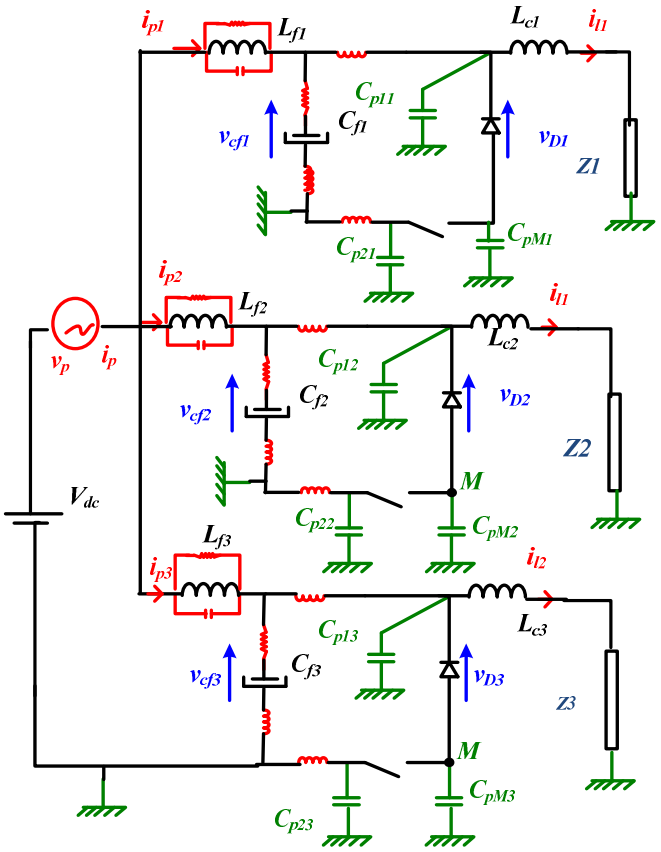

Fig 1 DC-DC converter cell

B. *Mathematical Modeling*

The model is realised by considering a switching function for each elementary converter $g_{sw}(t)$, defined in [11],[6], which is a periodic function where T_{sw} is a switching period for each.

The converters are identical and parallel with a control presented in (Fig. 2). The operation of modelling the converters, since the electrical signals are causal, the expression of the switching function is a product of convolution between The window function $\prod_{\alpha\frac{T_{sw}}{2}}(t)$ switching period and the Dirac $III_{Tsw}(t)$ [11], [6],[12], [13],[15].

The loads are taken in three types resistive, inductive and capacitive which can present a super capacitor

$$S_{out}(f) = \alpha \sum_{k=-\infty}^{+\infty} sinc(\pi\alpha k).e^{-j2\pi\frac{\alpha k}{2}}.S_{in}(f - kF_{sw}) \quad (4)$$

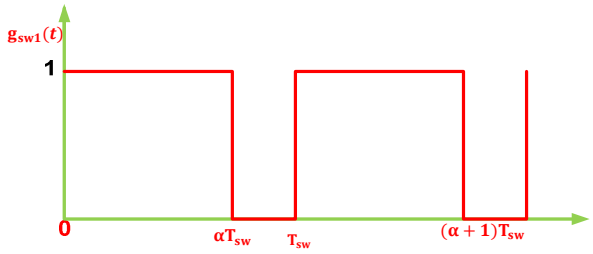

Fig 2 function switching

The operation of the converters is governed by the functioning of the switching cell (FIG. 3).

Which can take two states ("0 = off" or "1 = on"), on the controlled power device, depending on the duty cycle As shown in Fig. 2 supplied by the converter (Mosfet, IGBT ...), controlled by the switching function defined in FIG. 2. "L" is the line (or More in dc), "N" is the Neutral (or Minus in dc) and "G" is the Ground Fig 1and Fig2.

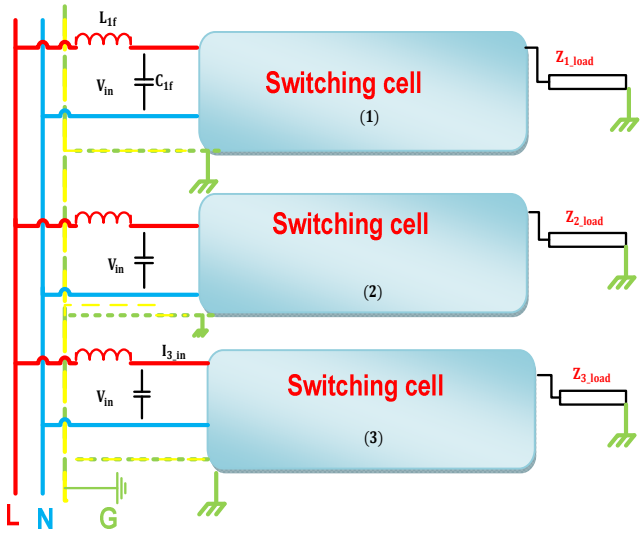

Figure 3 model electrical for converter's cell

$$Z_1(\omega_p) = R_c + L_c.\omega_p \quad (5)$$

$$Z_2(\omega_p) = R + 1/C_o.\omega_p \quad (6)$$

$$Z_3(\omega_p) = L_c.\omega_p + R_o \quad (7)$$

C. *Modelling of each Converter*

a) Resistive Load. [15]

$$Z_{DM\_R}=\frac{1+\frac{j\alpha^2.L_f}{R_c+j.L_c.p}+2.j.L_f.p\left[\sum_{q\neq 0}^{\infty}\frac{1-\cos(2.\pi.\alpha)}{(2.\pi.m)^2.(R_c+jL_c.(p-2.\pi.q.freq)}\right]+L_f.C_f.p^2}{j.p.C_f+\frac{\alpha^2}{R_c+jL_c.p}+2.\left[\sum_{m\neq 0}^{\infty}\frac{1-\cos(2.\pi.\alpha)}{(2.\pi.m)^2.(R_c+jL_c.(2.\pi.m.freq+p)}\right]} \quad (8)$$

b) Load capacity

$$Z_{DM\_C}=\frac{1+\frac{j.\alpha^2.L_f}{R+\frac{1-L_c.C_o.p^2}{j.C_o.p}}+2.j.L_f.p\left[\sum_{q\neq 0}^{\infty}\frac{1-\cos(2.\pi.\alpha)}{(2.\pi.m)^2.(R+\frac{1-L_c.C_o.(p-2.\pi.m.freq)^2}{j.C_o.(p-2.\pi.m.freq)}}\right]+L_f.C_f.p^2}{j.p.C_f+\frac{\alpha^2}{R+\frac{1-L_c.C_o.p^2}{j.C_o.p}}+2.\left[\sum_{m\neq 0}^{\infty}\frac{1-\cos(2.\pi.\alpha)}{(2.\pi.m)^2.(R+\frac{1-L_c.C_o.(2.\pi.m.freq+p)^2}{j.C_o.(2.\pi.m.freq+p)}}\right]} \quad (9)$$

c) Inductive load

$$Z_{DM\_L}=\frac{1+\frac{j.\alpha^2.L_f}{R_o++j.L_c.p}+2.j.L_f.p\left[\sum_{q\neq 0}^{\infty}\frac{1-\cos(2.\pi.\alpha)}{(2.\pi.m)^2.(R_o+j.L_c.(p-2.\pi.q.freq)}\right]+L_f.C_f.p^2}{j.p.C_f+\frac{\alpha^2}{R_o+j.L_c.p}+2.\left[\sum_{m\neq 0}^{\infty}\frac{1-\cos(2.\pi.\alpha)}{(2.\pi.m)^2.(R_o+j.L_c.(2.\pi.m.freq+p)}\right]} \quad (10)$$

This method is done by:

- Calculates for each impedance of the converter eq (8, 9,10).
- Calculates the equivalent impedance in parallel (13).

For ease of calculation, the parasitic elements are not introduced.

$$V_p(t)=Z_{DM}.i_p(t) \quad (11)$$

Of equation 1 and:

$$\frac{V_p(t)}{Z_{eqDM}}=\frac{V_p(t)}{Z_{RDM}}+\frac{V_p(t)}{Z_{CDM}}+\frac{V_p(t)}{Z_{LDM}} \quad (12)$$

$$\frac{1}{Z_{eqDM}}=\frac{1}{Z_{RDM}}+\frac{1}{Z_{CDM}}+\frac{1}{Z_{LDM}} \quad (13)$$

$$Z_{eqDM}=\frac{Z_{LDM}.Z_{RDM}.Z_{CDM}}{Z_{LDM}.Z_{RDM}+Z_{LDM}.Z_{CDM}+Z_{CDM}.Z_{RDM}} \quad (14)$$

After this result, we can say what a model equivalent to a converter's cell Fig 04.

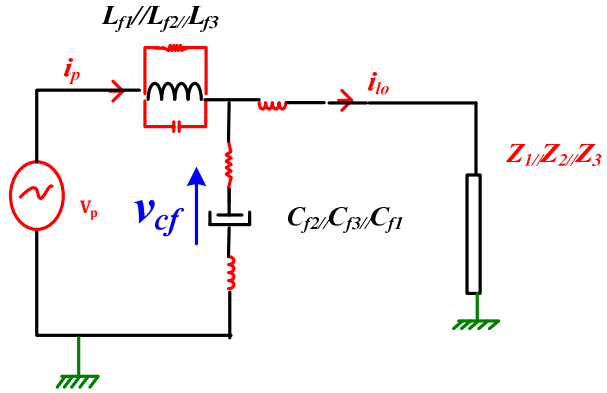

Figure 4 model equivalent to an converter's cell

III. PSPICE VALIDATION

The circuit is given in Fig.1 is simulated by PSpice.Converter components such as inductances capacitors and even the load are also characterised by Impedance Analyzer (Agilent 4294A) to introduce parasitical elements on the simulated circuit. An AC-source $v_p(t)$ is introduced to inject frequencies point by point from few Hertz up to 100MHz (Fig. 1). The DM impedance Z_{DM} is performed for each injected frequency as given by (1). Simulation parameters are given below:

- Switching frequency f_{sw} =10 kHz ,
- Duty cycle α = 0.5,
- Filter inductor L_f =30µH, pre(parallel resistive element)=2kΩ, pce (parallel capacitive,element)= 2pF,
- Filter capacitor C_f =100µF, sre (series resistive element)=230mΩ, sle(series inductive element)=30nH,
- Smoothing inductor L_o =1.61mH, pre=119.5kΩ, pce=79.6pF.
- Resistive load R_l =12.5Ω,
- Capacitive load C_o =100µF sre(300 mΩ).(proposed).
- inductive load L_o =1.61mH, sre 330 mΩ(proposed).

- Parasitical inductors layout L_p =10nH.

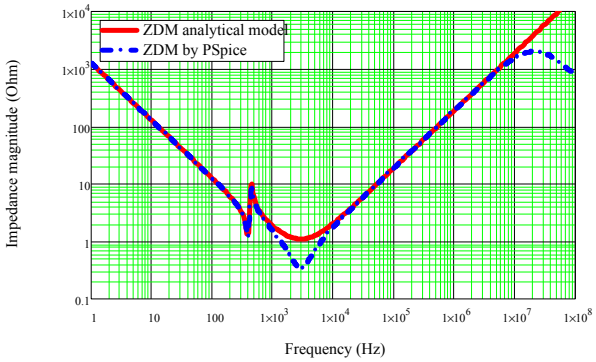

Fig 5 The red curve for the mathematical model and the blue for the simulation model (capacitive load).

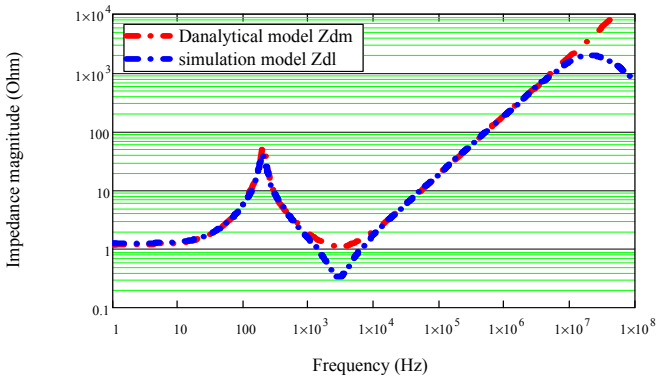

Fig 6 The red curve for the mathematical model and the blue for the simulation model (inductor load).

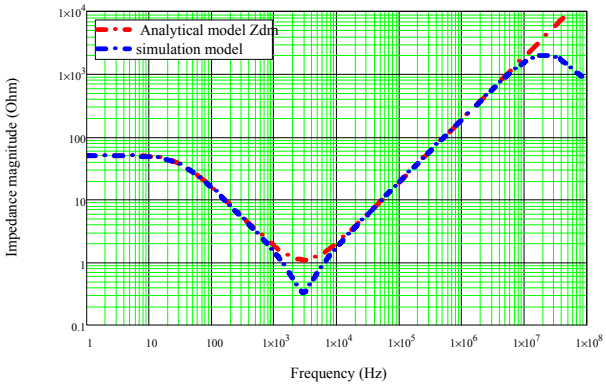

Fig 7 The red curve for the mathematical model and the blue for the simulation model (resistive load).

The diode has been modelled with a behavioural model using controlled sources, to consider various important phenomena as recovery, oscillations [14]. The simulation result is illustrated in Fig. 5,6,7,8,9.

That for both operating modes, offline Abbreviations and Acronyms. Moreover, online, ZDM and the input filter impedance is identical. It is worth noting the difference between the analytical computation and the other approach beyond 10MHz since the filter elements have been considered perfect.

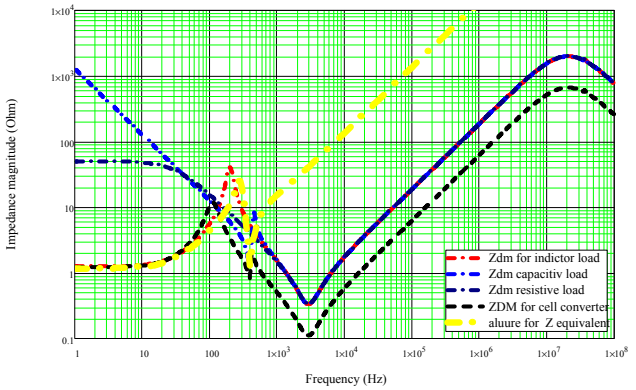

Fig 8 The curve red (inductor load) blue (capacitive load) brown (resistive load) black (Impedance of the system) yellow (Impedance equivalent).

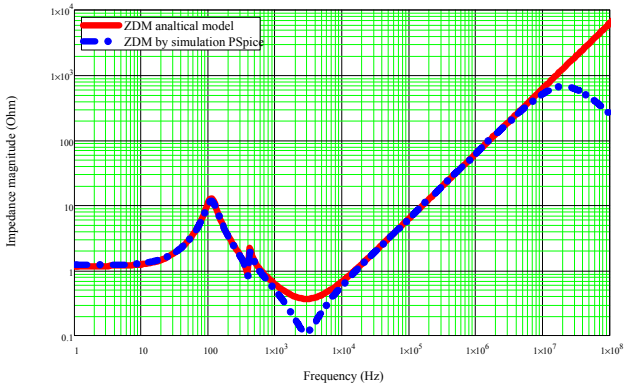

Figure 9 The red curve for the mathematical model and the blue for the simulation model (Impedance of the system).

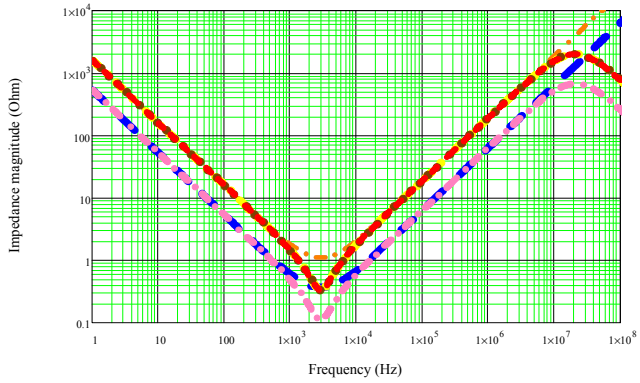

Fig 10 Impedance curves Mathematical model and offline simulation, purple and blue (simulation and analytical equivalent impedance) yellow, red, orange, is the impedances of the elementary, simulation and analytical

A. Discussion of Results

According to the theoretical study and the simulation, there are two frequency domains, low frequencies and high

frequencies.

• At low frequencies up to 100 Hz, all impedances depend on their loads.

• From 100 Hz to 900 Hz, resonances are observed between capacitances and inductances of the converter's cell.

• After this value, impedance patterns are the image of filters for all types of loads.

At the high frequency, the impedance of the converter cell is the impedance of the filters in parallel

• in height frequency, The impedance of the converter cell is the equivalent impedance of the impedances of the converters in parallel throughout the frequency range.

IV. CONCLUSION

In this paper, we have developed a mathematical model based on signal processing theory and circuit method to compute and predict the differential mode impedance of a converter cell from the impedance prediction of each elementary converter.

At low frequency, the impedance of the converter is just the reduced impedance at the output (load). PSpice Simulation also estimated the impedance in the two operating modes of the online and offline converter. The results obtained are in agreement with the proposed analytical approach solves the theory. The impedance DM of the converter is identical to the impedance of the high-frequency filter.

The impedance of the cell is the equivalent impedance of the converter put in parallel.

With its results in can reduce the filter by their location to the main power supply.

It should be noted that this study did not take into consideration certain parameters such as the influence of the connection (cable) and the location of the equipment which remains as a perspective of the others studies.

REFERENCES

[1] I. Cotton and A. Nelms, “Higher voltage aircraft power systems,” IEEEAerosp. Electron. Syst. Mag., vol. 23, no. 2, pp. 25–32, Feb. 2008.

[2] J. M. Poinsignon, P. Matossian, B. Mazari, and F. Duval, “Automotive equipment EMC modelling for electrical network disturbances prediction,” In Proc. IEEE Int. Symp. Electromagn. Compat., May 2003, vol. 1,pp. 415–417.

[3] M. Hartmann, H. Ertl, and J. W. Kolar, “EMI filter design for a 1 MHz,10 kW three-phase/level PWM rectifier,” IEEE Trans. Power Electron.,vol. 26, no. 4, pp. 1192–1204, Apr. 2011.

[4] B. Toure, J.-L. Schanen, L. Gerbaud, T. Meynard, J. Roudet, and R. Ruelland, “EMC modelling of drives for aircraft applications: Modelling process, EMI filter optimisation, and technological choice,” IEEE Trans. Power Electron., vol. 28, no. 3, pp. 1145–1156, Mar. 2013.

[5] V. Tarateeraseth, B. Hu, K. Yak See, and F. G. Canavero, “Accurate extraction of noise source impedance of an SMPS under operating conditions,” IEEE Trans. Power Electron., vol. 25, no. 1, pp. 111–117, Jan. 2009.

[6] A. ALES, JL. Schanen, D.Moussaoui, J. Roudet, "Impedances Identification of DC/DC Converters for Network EMC Analysis", IEEE Transactions on Power Electronics, Vol.PP , Issue: 99, page 1, 11 February 2014.

[7] M. Foissac, J. L. Schanen, and C. Vollaire, “Black box EMC model for power electronics converter,” in Proc. IEEE Energy Convers. Congr.Expo., Sep. 20–24, 2009, pp. 3609–3615.

[8] H. Bishnoi, A. C Baisden, P. Mattavelli, and D. Boroyevich, “Analysis of EMI terminal modelling of switched power converters,” IEEE Trans. Power Electron., vol. 27, no. 7, pp. 3924–3933, Sep. 2012.

[9] M. Ali, E. Laboure, F. Costa, and B. Revol, “Design of a hybrid integrated EMC filter for a DC–DC power converter,” IEEE Trans. Power Electron., vol. 27, no. 11, pp. 4380–4390, Jan. 2012.

[10] D. Labrousse, B. Revol, and F. Costa, “Common-mode modelling of the association of n-switching cells: Application to an electric-vehicle-drive System,” IEEE Trans. Power Electron., vol. 25, no. 11, pp. 2852–2859, Jun. 2010.

[11] A. ALES, JL. Schanen, D.Moussaoui, J. Roudet, "Experimental Validation of a Novel Analytical Approach about a DC-DC Converter Input Impedance", EPE'2013 ECCE Europe, Lille, France, Septembre 2013

[12] A.ALES, Z. Gouichiche, B. Karouche, D. Moussaoui, J-L. Schanen, J.Roudet, “The Accurate Input Impedances of DC-DC converters connected to the Network,“ 2015 IEEE 15th International Conference on Environment and Electrical Engineering (EEEIC), Rome 10-13 June 2015.

[13] A. Ales, M. A. Cherif Belhadj; D. Moussaoui; J-L. Schanen; J. Roudet" Analytical Models Synthesis of Power Electronic Converters", 16th International Conference on Environment and Electrical Engineering (EEEIC) 2016 Florence, Italy, June 2016

[14] C. Batard, D.M Smith, H. Zelaya, C.J Goodman, "New high power diode model with both forward and reverse recovery", Fifth International Conference on Power Electronics and Variable-Speed Drives, pp 447 - 452, 26-28 Oct 1994.

[15] A. Ales, G. Frantz, J-L. Schanen, D. Moussaoui, J. Roudet, "Input impedance investigation of a DC-DC converter on a large frequency range: a novel analytical approach", Power Electronics and Applications (EPE 2011), Sept 2013.